

Modeling and Hydrodynamic Characteristics of Bionic Undulate Fin Propeller Driven by Hydraulic System

XU Hai-jun¹

PAN Cun-yun²

XU Xiao-jun³

ZHOU Han⁴

Abstract: The bionic undulating propeller driven by hydraulic system has different structure, kinematic and dynamic characteristics than that of the common bionic undulating propellers driven by other sources. This paper highlights firstly the structure and driving mechanism of bionic undulating propeller with a hydraulic system, and then setup its kinematic model, based on ruled-surface equation. Changing rules of dynamic mesh for bionic fin is designed based on kinetic model. Later on, the changing courses of hydrodynamic force caused by the bionic undulating fin are calculated and studied with the CFD (Computational Fluid Dynamics) method, as well as the changing characteristics of the fluid pressure field. The analysis showed that while driven by hydraulic system, the bionic propeller could produce full-baseline undulating motion, and has flexible start-up process, as well as doubled-frequency character. The bionic undulating fin driven by hydraulic system puts up flexible characters on both kinematic and dynamics.

Key Words: Hydraulic Driven; Undulating Fin; Bionic Propeller; Dynamic Mesh; Hydrodynamics

1. INTRODUCTION

¹Lecturer, College of Mechatronics Engineering and Automation, National University of Defense Technology, Changsha, Hunan 410073, China.

² College of Mechatronics Engineering and Automation, National University of Defense Technology, Changsha, Hunan 410073, China.

³ College of Mechatronics Engineering and Automation, National University of Defense Technology, Changsha, Hunan 410073, China.

⁴ College of Mechatronics Engineering and Automation, National University of Defense Technology, Changsha, Hunan 410073, China.

*Received 8 May 2010; accepted July 2 2010

Bionic propelling technology has gained much attention from researchers around the world. However, as for the study of undulating mechanism and engineering technology, little work has been put on existing bionic undulating propellers, which leads to the distance on motion and propelling ability between expected and actual bionic propellers, and bionic of fish (Maciver et al., 2004; LIU & HU, 2006; XIE et al., 2006)

In order to enhance the flexible characteristics of structure and motion in bionic propeller, the paper designs a bionic undulating propeller with a pump-valve controlled hydraulic system, called HBUP (Hydraulic Driven Bionic Undulating Propeller). The HBUP consisted of bracket, RDV (Rotational Direction Valve), several BSUs (Bionic Swaying Units) and bionic fin (ZHANG et al., 2008), as is shown in figure 1.

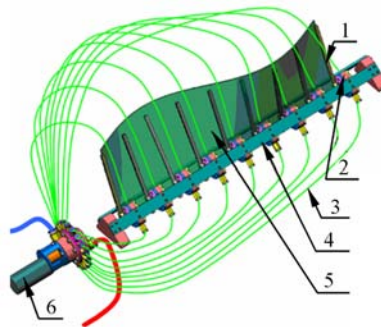


Figure 1: Structure of Hydraulic driven Bionic Undulating Fin

(1) Bionic Ribbing (2) Bionic Swaying Unit (3) Branch Oil Pipe (4) Bracket (5) Bionic Fin (6) Rotational Direction Valve

The RDV drives each BSU swaying to and fro, periodically, and restricts several BSUs swaying in sequence, create undulating wave, with controlled spreading frequency and direction. By changing oil flux, swaying range can be adjusted, and similarity is the undulating wave amplitude. The HBUP could produce variable wave length under different connection method between RDV and BSUs.

2. KINEMATIC MODELING OF HBUP

2.1 Setup of Reference Frames

To be convenient for modeling and analyzing, several reference frames are setup (YAN, 2005), as shown in figure 2.

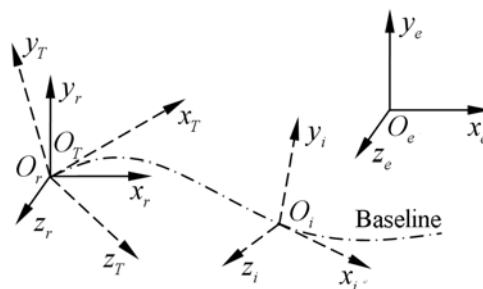


Figure 2: Setup of Reference Frames for HBUP

Base-point Frames $O_i x_i y_i z_i$. Origin O_i is the base-point of the BSU i , axis x_i towards the tangent direction of base-line at point O_i , axis y_i towards the main normal direction, and axis z_i towards the sub-normal direction, then reference frames $O_i x_i y_i z_i$ are setup.

HBUP Frame $O_T x_T y_T z_T$. It has superposition to the first base-point frame.

HBUP Accompanying Frame $O_r x_r y_r z_r$. It has superposition to HBUP Frame at the initial time $t = 0s$.

The Inertial Frame $O_e x_e y_e z_e$. Origin O_e fixed to the ground, and axis x_e, y_e, z_e parallel to axis x_r, y_r, z_r .

2.2 Kinematic Modeling of HBUP

In figure 3, P is a common point on bionic fin Ω in HBUP Frame $O_T x_T y_T z_T$, $\overline{O_p P_e}$ stands for the ribbing across P from top-point P_e to base-point O_p , with the coordinates $\vec{a}(x) = [x, y(x), 0]^T$, and $\|\overline{O_p P_e}\| = h(x)$. According to the Base-point Frames, base-point frame $O_p x_p y_p z_p$ is setup for ribbing $O_p P_e$, then $\theta(x, t)$ is angle between $\overline{O_p P_e}$ and axis y_p .

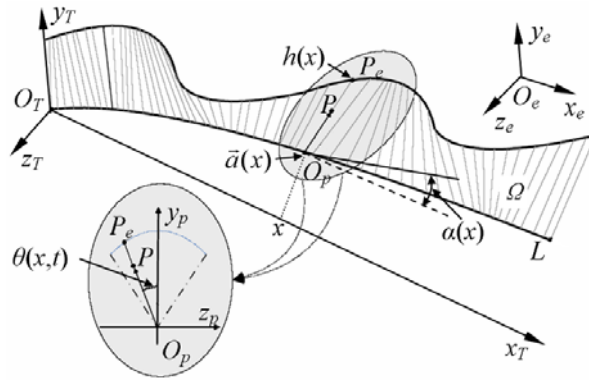


Figure 3: Ruled-surface Kinematic Model for Bionic Fin (HU et al., 2009)

Defining the variable $s \in [0, 1]$ along ribbing, and $\|\overline{O_p P}\| = s \cdot h(x)$. Then coordinates of P in $O_p x_p y_p z_p$ can be depicted by following formula.

$$\begin{cases} x_p = 0 \\ y_p = s \cdot h(x) \cdot \cos \theta(x, t) \\ z_p = -s \cdot h(x) \cdot \sin \theta(x, t) \end{cases} \quad (1)$$

When baseline is supposed as a planar curve, then $\overline{O_T O_p}$ in $O_T x_T y_T z_T$ can be described as follows.

$$\overline{O_T O_p} = \vec{a}(x) = \begin{bmatrix} x \\ y(x) \\ 0 \end{bmatrix} = \begin{bmatrix} x \\ a_1 x^2 + a_2 x + a_3 \\ 0 \end{bmatrix} \quad (2)$$

Where, $a_i (i = 1, 2, 3)$ are constant.

Letting the angle between tangent of baseline at O_p and axis x_T as $\alpha(x)$, then $\alpha(x) = \arctan y'(x)$.

Thus $\overline{O_p P_e}$ can be explained in $O_T x_T y_T z_T$ as follows:

$$\overline{O_p P_e} = \begin{bmatrix} \cos \alpha(x) & \sin \alpha(x) & 0 \\ -\sin \alpha(x) & \cos \alpha(x) & 0 \\ 0 & 0 & 1 \end{bmatrix} \cdot \begin{bmatrix} x_p \\ y_p \\ z_p \end{bmatrix} = \begin{bmatrix} s \cdot h(x) \cdot \cos \theta(x, t) \cdot \sin \alpha(x) \\ s \cdot h(x) \cdot \cos \theta(x, t) \cdot \cos \alpha(x) \\ -s \cdot h(x) \cdot \sin \theta(x, t) \end{bmatrix} \quad (3)$$

According to relative bionics study (DONG, 2003), changing rules of ribbing length can be summarized into the following form:

$$h(x) = h_1 \cdot x^2 + h_2 \cdot x + h_3 \quad (4)$$

Where, $h_i (i = 1, 2, 3)$ are constant, and not all of them are zero.

Combined with equation (1) ~ (4), coordinates of P in $O_T x_T y_T z_T$ is shown as follows.

$$\begin{aligned} \vec{r}_p(x, s, t) &= \vec{a}(x) + s \cdot h(x) \cdot \vec{c}(x, t) \\ &= \begin{bmatrix} x \\ a_1 x^2 + a_2 x + a_3 \\ 0 \end{bmatrix} + s \cdot (h_1 \cdot x^2 + h_2 \cdot x + h_3) \cdot \begin{bmatrix} \cos \theta(x, t) \cdot \sin \alpha(x) \\ \cos \theta(x, t) \cdot \cos \alpha(x) \\ -\sin \theta(x, t) \end{bmatrix} \end{aligned} \quad (5)$$

Where, $\vec{c}(x, t)$ is the transforming matrix from $O_p x_p y_p z_p$ to $O_T x_T y_T z_T$. When P moves freely on the whole bionic fin Ω , equation (5) depicts the undulating motion shape of the whole bionic propeller at any time.

3. HYDRODYNAMIC MODEL AND PARAMETER SETTING OF HBUP

3.1 Parameter Setting of Hydrodynamic model

A three-dimensional model of bionic fin is built, according to the parameters in table 1.

Table 1: Structure and Motion Parameters of Bionic Fin

Parameter	Height (H)	Wavelength(λ)	Frequency(f_w)	Amplitude(θ_{max})
Unit	m	m	Hz	rad
Value	0.2	0.6	3	$\pi/12$

Supposing that non-slippage condition is permitted on the undulating wave surface of bionic fin, which means that the velocity of fluid nearby the surface is equal to that of mesh grid node. Besides, assumptions are made that fluid is incompressible with infinite volume, and the fluid field is still until the bionic fin starts moving (HAN et al., 2004; WANG, 2008). Parameters of the calculating region for bionic fin are as follow:

(1) Sizes of calculating region and dense region are set as follows.

$$\begin{cases} L \times W \times H = 4m \times 2m \times 2m \\ L_1 \times W_1 \times H_1 = 1.6m \times 0.8m \times 0.8m \end{cases} \quad (6)$$

(2) Entrance boundary conditions: initial velocity and pressure of fluid are zero.

$$\begin{cases} \vec{V}_{in} = [v_x \quad v_y \quad v_z]^T = [0 \quad 0 \quad 0]^T \\ p_{in} = 0 \end{cases} \quad (7)$$

(3) Exit boundary conditions: velocity and pressure grads of fluid are zero.

$$\begin{cases} \frac{\partial \vec{V}_{out}}{\partial x} = \frac{\partial \vec{V}_{out}}{\partial y} = \frac{\partial \vec{V}_{out}}{\partial z} = 0 \\ \frac{\partial p_{out}}{\partial x} = \frac{\partial p_{out}}{\partial y} = \frac{\partial p_{out}}{\partial z} = 0 \end{cases} \quad (8)$$

Parameters of calculating region are shown in figure 4.

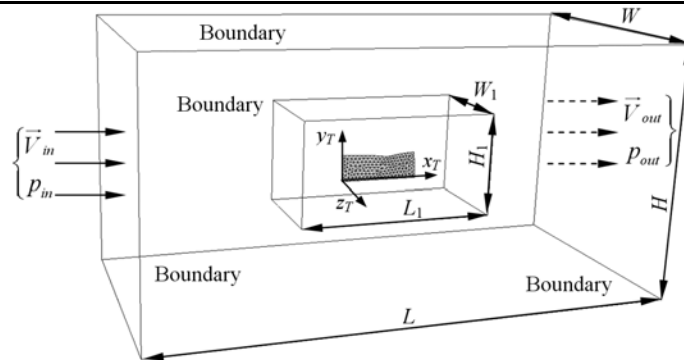


Figure 4: Parameters Setting of Calculating Region

3.2 Mesh Grid Dividing of Calculating Region

In order to capture effectively the fluid information while the bionic fin is undulating, mesh grid forming method with multi-sized function is used to make a balance between mesh grid size and number. This can be explained as follows: Dense region near bionic fin changes rapidly and it is divided into tetrahedron mesh grid with tiny size. However, calculating region far away from bionic fin can be divided into tetrahedron mesh grid too, but with larger size (ZHOU, 2009).

With the mesh grid generating method above, mesh effect of calculating region is shown in figure 5, after a horizontal plane is used to intercept the calculating region.

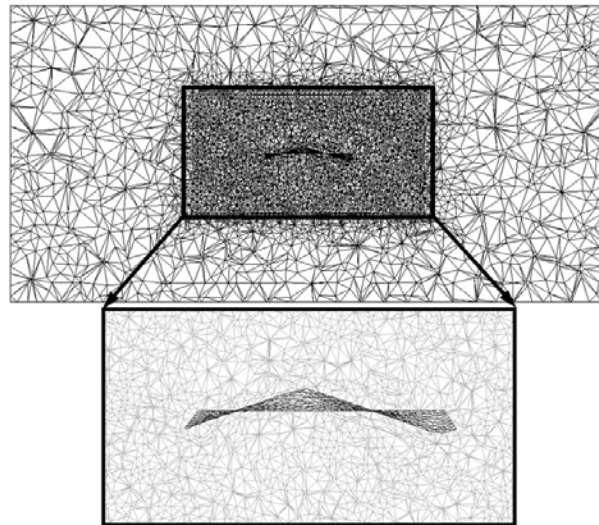


Figure 5: Mesh grid dividing of Calculating Region

4. HYDRODYNAMICS ANALYZING OF HBUP

4.1 Analyzing of Hydrodynamic Forces and Torques

When calculating in the software Fluent, bionic fin model is fixed by its baseline, and the iterative time step is 0.01s. Starting and stable process is set as follows: during starting process, the undulating frequency keeps $f_w = 3\text{Hz}$, and undulating amplitude increases from zero to $\pi/12$. Within three motion cycles, the model keeps undulating under constant motion parameters for another three motion cycles.

According to the calculating results during the starting and stable process of bionic fin, curves of hydrodynamic forces in three directions of $O_T x_T y_T z_T$ are shown in figure 6.

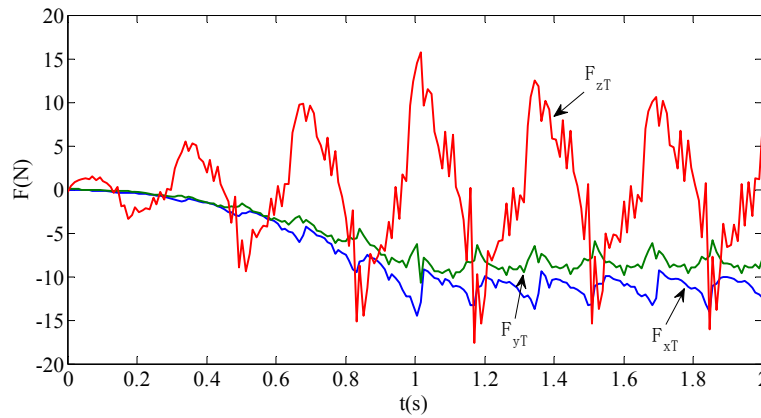


Figure 6: Curves of Hydrodynamic Forces

As is shown in figure 6, during the starting and stable processes ($t = 0 \sim 2s$), hydrodynamic forces generate along each axis of $O_T x_T y_T z_T$, and appear periodicity obviously. Minus values mean that directions of hydrodynamic forces are opposite to that of undulating motion.

Propelling and lifting forces along axis x_T and y_T increase following the increase of undulating amplitude until it achieves stability ($t=1 \sim 2s$), maximal values of $|F_{x_T}|$ and $|F_{y_T}|$ are $14.4639N$ and $10.7308N$ respectively, periodical average values are $|\bar{F}_{x_T}| \approx 8.0682N$ and $|\bar{F}_{y_T}| \approx 6.1412N$ respectively. Changing cycle of propelling and lifting forces are nearly of the same magnitude, about $0.1626s$, which is about half of the undulating cycle. This means that the changing frequencies of propelling and lifting forces are twice in magnitude of that of undulating motion.

Periodical average value of lateral force along axis z_T is about $|\bar{F}_{z_T}| \approx 0.1686N$, far away from propelling and lifting forces. However, changing cycle of lateral force is about $0.3184s$, equal to that of undulating cycle.

The changing frequencies of propelling and lifting forces are twice in magnitude of that of undulating motion. This phenomena is called doubled-frequency effect of undulating. Although periodical average value of lateral force is very small and is disadvantage of undulating motion, since it exists all the time.

With the same calculating results, curves of hydrodynamic torques in three directions of $O_T x_T y_T z_T$ are shown in figure 7.

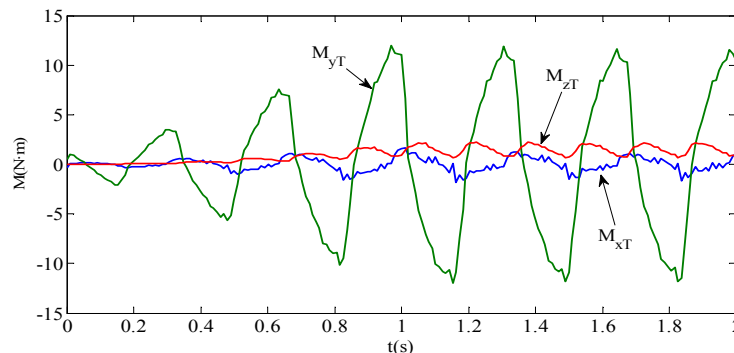


Figure 7: Curves of Hydrodynamic Torques

As is shown in figure 7, periodical average value of rolling torque along axis x_T and yawing torque along axis y_T are nearly zero, and the changing cycles are about 0.3262s, nearly the same of undulating cycle. This is because rolling and yawing torques come from the action of lateral force F_{z_T} .

Maximal value and periodical average value of pitching torques along axis z_T are $M_{z_T} \approx 2.2539N \cdot m$ and $\bar{M}_{z_T} \approx 1.0793N \cdot m$ respectively, the changing cycle is about 0.1607s, nearly half of the undulating cycle. Therefore, there is doubled-frequency effect for the pitching torque two. This is because pitching torque mainly comes from F_{x_T} and F_{y_T} , where doubled-frequency effects exist.

4.2 Characteristics of Pressure Field in Stable Process

After visualization on the calculated results, changing course of pressure field on bionic fin is obtained, as shown in figure 8. It is obvious that there are both high and low pressure regions on bionic fin synchronously. These two kinds of pressure regions change and alternate regularly into one direction, along with the spreading of undulating wave.

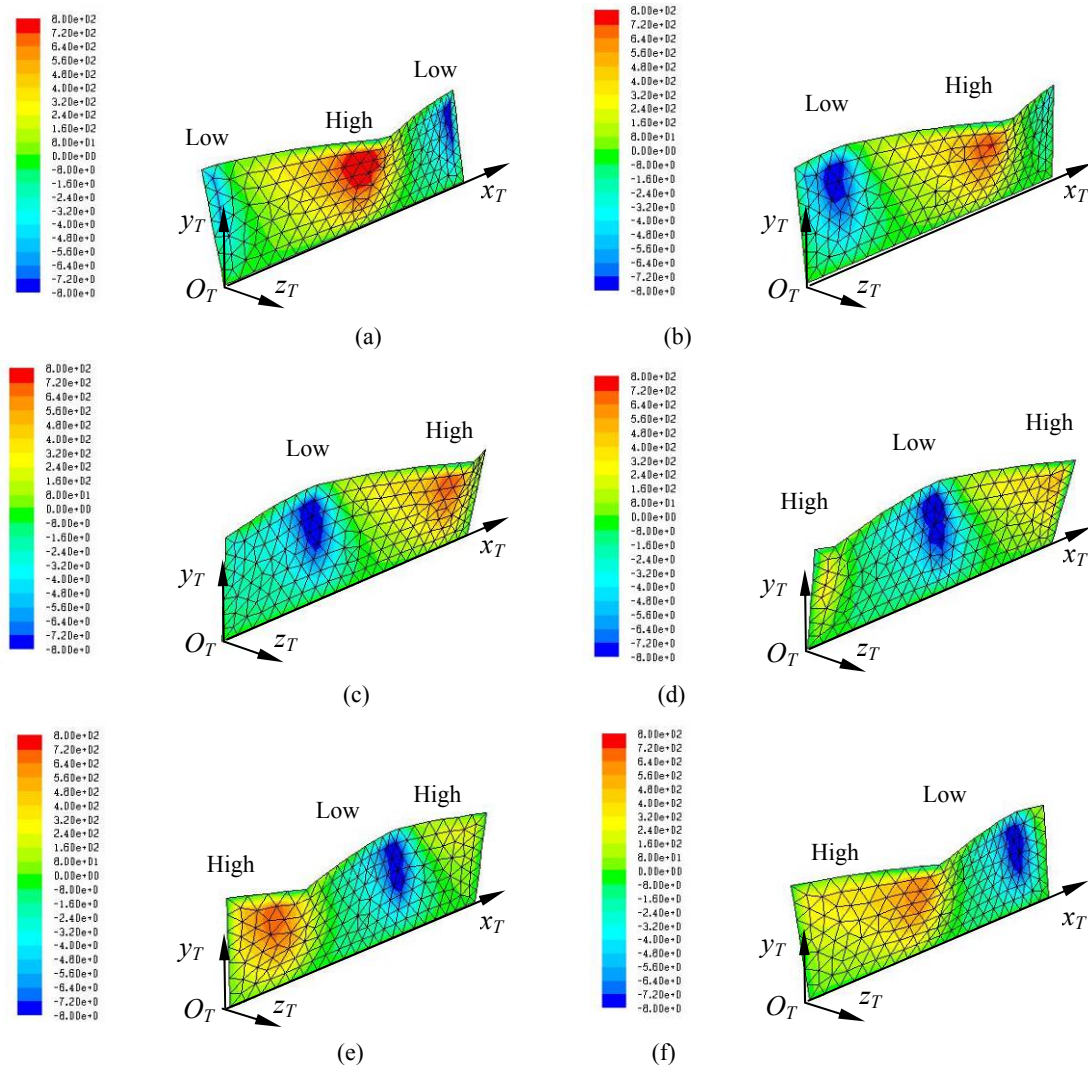


Figure 8: Pressure Nephogram on Bionic Fin in an Undulating Cycle

The undulating waves spreads along axis x_r , followed by low and high pressure regions moving from front to back in sequence and periodically, as shown in figure 8, and cause hydrodynamic forces and torques. In a single undulating cycle, low and high pressure regions change their position twice in turn, then form the doubled-frequency effect

5. CONCLUSIONS

The bionic undulate propeller using hydraulic system as driving chain could generate an undulating motion with amplitude gradually increasing, so that the hydrodynamic forces and torques increase inchmeal. This makes the bionic structure carry hydro-load gradually, which is uniform to that of nature fish.

Some of the hydrodynamic forces and torques are of doubled-frequency characteristic, because of the trade off between low and high pressure regions on undulating bionic fin.

It is obvious that hydraulic system provides the bionic propeller unique flexible structure and dynamic characteristics, which are very important in underwater bionic propelling technology.

REFERENCES

- DONG Zengfu. (2003). Matrix Analysis Course[M]. HaErBin: HaErBin Industry University Press. (In Chinese)
- HAN Zhanzhong, WANG Jing, LAN Xiaoping. (2004). Calculating Examples and application of Fluid Engineering Simulation in Fluent[M]. Beijing: Beijing Institute of Technology Press. (In Chinese)
- HU Tianjiang, SHEN Lincheng, LIN Longxin, XU Haijun. (2009). Biological inspirations, kinematics modeling, mechanism design and experiments on an undulating robotic fin inspired by *Gymnarchus niloticus*. Mechanism and Machine Theory. 44(3): 633-645. (In Chinese)
- LIU J., HU H. (2006). Biologically inspired behaviour design for autonomous robotic fish[J]. International Journal of Automation and Computing. 3(4): 336-347. (In Chinese)
- Maciver M. A., Fontaine E., Burdick J. W. (2004). Designing Future Underwater Vehicles: Principles and Mechanisms of the Weakly Electric Fish[J]. IEEE Journal of Oceanic Engineering. 39(3): 651-659.
- WANG Fujun. (2008). Computational Fluid Dynamics Analysis-CFD mechanism and application[M]. Beijing: Tsinghua University Press. (In Chinese)
- XIE Haibin, SHEN Lincheng, ZHANG Daibing. (2006). Dynamic Analysis of Undulatory Propulsion of Long Flexible Fin. Mechanics in Engineering. 28(4): 14-19. (In Chinese)
- YAN Weisheng. (2005). Fish Torpedo Navigation Dynamics[M]. Northwest University of Technology Press. (In Chinese)
- ZHANG Daibing, XIE Haibin, SHEN Lincheng. (2008). A Bionic Underwater Thruster of Undulate Fin Driven by Hydraulic System. China. 200810031901.1[P].2008-7-28. (In Chinese)
- ZHOU Han. (2009). Dynamics Behavior and Experimental Research of Bionic Underwater Vehicle Propelled by Undulatory Fins[D]. Changsha: National University of Defense Technology. (In Chinese)